Meteorol. Atmos. Phys. 74, 1–9 (2000)

Meteorology and Atmospheric Physics

Lab of Ocean Circulation and Air-sea Interaction, Institute of Oceanology, Chinese Academy of Sciences Qingdao, P.R. China

Equatorial pacific SSTA-related decadal variations of potential predictability of ENSO and interannual climate

A. Wu and **D. Hu**

With 7 Figures

Received October 19, 1999
Revised December 30, 1999

Summary

Based on analysis of NCEP reanalysis data and SST indices of the recent 50 years, decadal changes of the potential predictability of ENSO and interannual climate anomalies were investigated. Autocorrelation of Nino3 SST anomalies (SSTA) and correlation between atmospheric anomalies fields and Nino3 SSTA exhibit obvious variation in different decades, which indicates that Nino3 SSTA-related potential predictability of ENSO and interannual climate anomalies has significant decadal changes. Time around 1977 is not only a shift point of climate on the interdecadal time scale but also a catastrophe point of potential predictability of ENSO and interannual climate. As a whole, ENSO and the PNA pattern in boreal winter are more predictable in 1980s than in 1960s and 1970s, while the Nino3 SSTA-related potential predictability of the Indian monsoon and the East Asian Monsoon is lower in 1980s than in 1960s and 1970s.

1. Introduction

El Niño-Southern Oscillation (ENSO) is the strongest climate signal on interannual timescale, which is characteristic of irregular re-appearance of anomalous warm or cold water in the central-eastern tropical Pacific once a few years. Although ENSO originates in the tropical Pacific, it affects not only regional but also global climate (Wallace et al., 1981, 1998; Trenberth et al., 1998). Previous studies show that, if SST can be predicted rather well, seasonal-to-interannual climate will be foretold in a great success. In other words, to large extent, the climate is predictable (CLIVAR-1996). It is usually called the SST-related potential predictability of climate, since SST is assumed to be able to be predicted successfully in advance.

The most significant variablity of the tropical Pacific SST is interannual, usually of 3∼7 years (Barnett et al., 1991). However, if a long time series of the tropical Pacific SST is examined with wavelet analysis, variability of lower frequency with period longer than 10 years can be easily found. Interdecadal timescale signals of SST exist not only in the tropical Pacific, but also in the North Pacific of middle latitudes (Qian et al., 1998). Also El Niño-events in different decades have different characteristics in their phases of onset, development and decay (Wang, 1995; Gu and Philander, 1995). For most El Niño events before 1980, warming of the equatorial Pacific usually started from the coast of South America in spring and then extended westward, while for those after 1980, warming of the equatorial Pacific appeared first in the western equatorial Pacific and then propagated eastward. For 1990s, a new feature of El Niño events is found, which is of shorter interval between two events and warm events are dominant. And what is more, the most recent El Niño of 1997/98 is, by some measures, the strongest on record (McPhaden, 1999). In terms of predictive capability, most

models exhibit obvious dependence of skill on decade as reviewed by Latif et al. (1998). Ji et al. (1996) and Chen et al. (1995) pointed out that the predictive capability for 1990s' ENSO events is considerably poorer than for 1980s'. And the predictive capability for 1980s' ENSO events is much higher than for 1970s' (Flugel et al., 1998). Balmaseda et al. (1995) investigated the autocorrelation of the tropical Pacific-SST anomalies and found that seasonal dependence of prediction skill was strong in 1970s and weak in 1980s. The forecast skill seemed to be affected by the extent of seasonal dependence of autocorrelation of the tropical Pacific-SST anomalies.

It should be noted that forecast results depend on both the predictive capability of models and the predictability of ENSO or climate system. With the same model, it is easier to make a successful forecast in a decade of higher predictability. Climate predictability is attributed to many factors, of which SST is the most important one. The main aim of AMIP (Atmosphere Model Intercomparison Project) initiated in 1990 is to compare the simulation capability of AGCMs forced by observed SST and sea ice, at the same time, to investigate the potential predictability of the global climate (WCRP-92). Strictly speaking, the potential predictability is an intrinsic characteristic of the climate system and does not depend on what models are used. However, it can be reflected from the model results. In the present paper, instead of using numerical modeling, a statistical correlation analysis of observed data is adopted to study the SSTA-related potential predictability of ENSO and interannual climate anomalies.

This paper is arranged as follow. Section 2 describes data and analysis methods. Section 3 discusses decadal variation of potential predictability of ENSO. The Nino3 SSTA-related potential predictability of the interannual climate anomalies over the Pacific-Northern America and Asian monsoon areas is investigated in Sect. 4. Section 5 is devoted to concluding remarks.

2. Data and methods

a. Data

1) COADS monthly SST anomalies from 1945 to 1993 with $1^\circ \times 1^\circ$ grid covering the global ocean and their corresponding climatological mean.
2) Global monthly winds at 200hPa, 850hPa and geopotential height at 500hPa from 1949 to 1998 with grid of $2.5^\circ \times 2.5^\circ$ from NCEP reanalysis.
3) Monthly Nino3 SST indices from January of 1950 to April of 1999, which were download from *http://www.cpc.ncep.noaa.gov/data/indices*.

b. Methods

1) In addition to *Nino3 index* which is defined as the area-averaged SST anomalies within the region of 150° W $\sim 90^\circ$ W, 5° S $\sim 5^\circ$ N in the central-eastern equatorial Pacific, other atmospheric indices were calculated.

(i) *TW2 index* is defined as the area-averaged zonal wind anomalies at 850hPa within the region of $180^\circ \sim 140^\circ$ W, 5° S $\sim 5^\circ$ N in the central equatorial Pacific.

(ii) *PNA index* is defined as following:

$$PNA = 0.25 * [z^*(20^\circ \mathrm{N}, 160^\circ \mathrm{W}) - z^*(45^\circ \mathrm{N}, 165^\circ \mathrm{W}) + z^*(55^\circ \mathrm{N}, 115^\circ \mathrm{W}) - z^*(30^\circ \mathrm{N}, 85^\circ \mathrm{W})],$$

where z^* is the height anomaly at 500hPa in boreal winter (Ni, 1993).

(iii) The Indian Monsoon Index (*INMI*) is defined as the area-averaged zonal wind shear between 200hPa and 850hPa within the Indian summer monsoon area of 40° E $\sim 80^\circ$ E, 5° N $\sim 20^\circ$ N (Webster and Yang, 1995),

$$INMI = \mathrm{ave}(u_{850\mathrm{hPa}} - u_{200\mathrm{hPa}}).$$

(iv) The East Asian monsoon index (*EAMI*) is defined as the area-averaged meridional wind at 850hPa within the East Asian monsoon area of 110° E $\sim 130^\circ$ E, 20° N $\sim 40^\circ$ N (Zhang et al., 1996),

$$EAMI = \mathrm{ave}(v_{850\mathrm{hPa}}).$$

If summer (winter) wind is used, then we can get the East Asian summer (winter) monsoon Index – $EAMI_{\mathrm{sum}}(EAMI_{\mathrm{win}})$.

2) Main method in this study is correlation analysis. Suppose we have a variable ξ, the lagged or contemporary correlation between

ξ and *Nino3 index* can represent the Nino3 SSTA-related potential predictability of ξ. The higher correlation is, the more predictable ξ is. Moreover, to discuss the decadal changes of interannual climate predictability, moving-window correlation technique is used.

3. Decadal Variation of potential predictability of ENSO

a. Persistence predictability of Nino3 SSTA

Nino3 index is widely used to depict the El Nino(or La Nina)-events and often used as a predictand of ENSO prediction (Barnett, 1991, Cane et al., 1986). Monthly *Nino3 index* from January of 1950 to April of 1999 is smoothed with 9-year running averaging and filtered with a low-pass filter retaining variability with period longer than 9 years. The results are depicted with the solid line and thick dashed line in Fig. 1a, respectively, where interdecadal variation of the equatorial Pacific SST can be obviously seen. On interdecadal timescale, Nino3 SSTA is basically negative before 1977 except for the weak positive value in late 1960s and positive after 1977. Two warm peaks appear in early 1980s and late 1990s, respectively. The amplitude of the latter one reaches 0.6 °C.

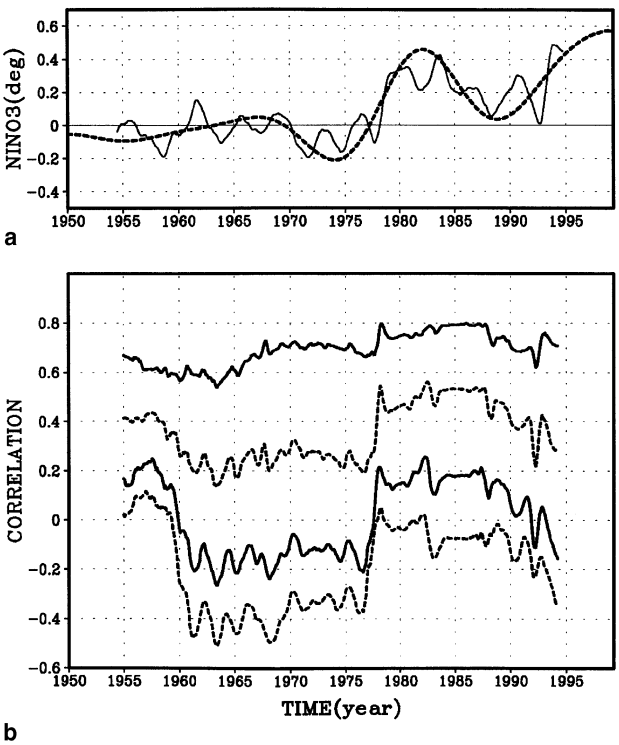

Fig. 1a. 9-year running average and low-pass-filtered series of *Nino3 index* on interdecadal timescale shown with the solid line and the thick dashed line, respectively; **b.** Moving-window autocorrelation of *Nino3 index*. The length of window is 121 months and the 4 lines from top to bottom represent the lagged time of two *Nino3 index* series is 3, 6, 9 and 12 months successivley

Fig. 1b shows the moving-window autocorrelation of *Nino3 index*. The length of moving-window is 121 months ($\approx$10 years) and the 4 lines in Fig. 1b from top to bottom represent that the lagged time of two *Nino3 index* series is 3, 6, 9 and 12 months successively. The autocorrelation, in fact, indicates the persistence of Nino3 SST, therefore it can also be considered as a kind of previous-SST-related potential predictability of SST in the equatorial Pacific. It can be seen from Fig. 1b that 4 lines have similar time variation despite of different values. After a drop in late 1950s, correlation coefficient is relatively low from early 1960s to 1976. It is notable that there is an abrupt increase for each line around 1977. Correlation after 1978 (including 1980s) is relatively high, but it tends to decline after 1990. Therefore, the persistence predictability of Nino3 SST in 1980s is relatively higher than that in 1960s, 1970s and 1990s. A catastrophe point of the potential predictability is near 1977 when Nino3 SST shifts from cold to warm on interdecadal timescale (see Fig. 1a).

b. Potential predictability of ENSO

The interaction between the tropical Pacific wind anomalies, especially the zonal surface wind anomalies and the equatorial SST anomalies is critical for ENSO processes. The correlation between wind anomalies and SST anomalies can, to some extent, reflect the potential predictability of ENSO.

With zonal wind at 850hPa from NCEP reanalysis data, *TW2 index* is calculated. From either the 9-year-running-averaged series (solid line in Fig. 2a) or the low-pass-filtered series (thick dashed line) of *TW2 index*, it can be clearly seen that the tropical Pacific wind possesses significant variation on interdecadal timescale, which resembles to that of *Nino3 index* shown in Fig. 1a. It is basically easterly anomalies before 1977 and westerly anomalies

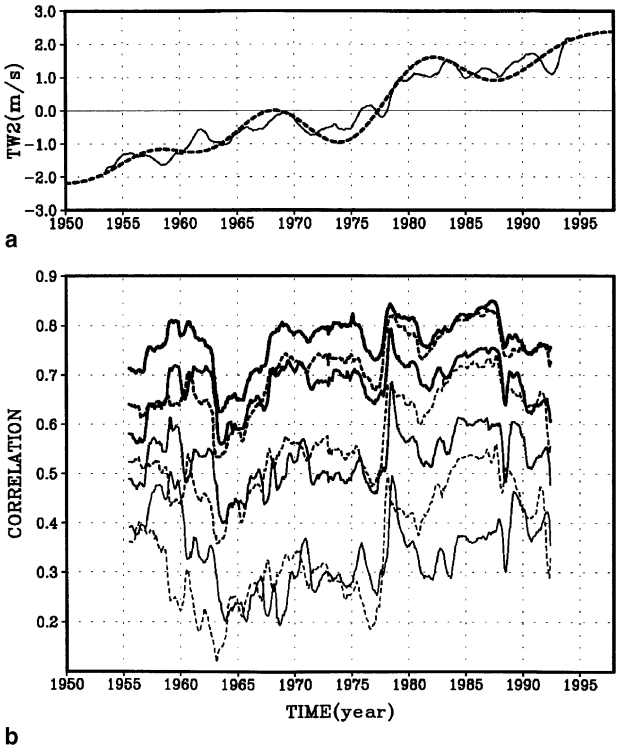

Fig. 2a. 9-year running average and low-pass-filtered series of *TW2 index* on interdecadal timescale shown with the solid line and thick dashed line, respectively; **b.** Moving-window correlation between *TW2 index* and *Nino3 index*. The length of window is 121 months. 4 solid lines from top to bottom represent wind anomalies lags SSTA 0, 2, 4, 6 months successively and 3 dashed lines from top to bottom represent wind leads SSTA 2, 4, 6 months succesively

after 1977. The strong westerly anomalies after 1900 can exceed 2 m/s. Obviously, the existence of westerly anomalies is favorable for the onset and development of El Niño. The high-frequency-appearance of El Niño-events in 1990s might have close relationship with this.

Moving-window correlation between *TW2 index* and *Nino3 index* is calculated and shown in Fig. 2b. The length of moving-window is 121 months. In Fig. 2b, 4 solid lines from top to bottom represent wind anomalies lags SSTA 0, 2, 4, 6 months successively and 3 dashed lines from top to bottom represent wind leads SSTA 2, 4, 6 months successively. For each line, it can be found that there is a decline in early 1960s. Then the correlation coefficient increases slowly with fluctuation around a relatively low level. An abrupt increase of correlation takes place around 1977. Relatively high correlation maintains from 1978 to 1988, then tends to decline in 1990s. Therefore, both the led and lagged correlation indicate that ENSO events are more potentially predictable in 1980s than in other decdal periods of the recent 40 years. This phenomenon was also found in the predictive skill of many ENSO prediction models (Balmaseda et al., 1995; Latif et al., 1998).

Two 15-year periods are selected: 1960–74 and 1978–92. These two periods correspond to the cold and warm phases on interdecadal timescale, respectively (see Fig. 1a). The correlation of monthly zonal wind anomalies at 850hPa and *Nino3 index* during each 15-year period is calculated (sample number is 180). As shown in Fig. 3, seven panels from top to bottom represent SSTA leads wind anomalies 6, 4, 2, 0 months, SSTA lags wind anomalies 2, 4, 6 months successively. The left column represents the 1960–74 period and the right column represents the 1978–92 period. Areas with the correlation coefficient larger than 0.5 are shaded. From here we can see that positive correlation basically appears in the equatorial Pacific. Positive correlation coefficient in the right column is always higher and wider than in the left column, which suggests that the potential predictability of ENSO during 1978–92 is higher than that during 1960–74. In addition, from bottom to top, positive correlation in the right column exhibits clearly eastward propagation, while the eastward propagation in the left column is not obvious, especially when SSTA leads wind anomalies. The center of positive correlation weakens and moves westward in the upper 3 panels of the left column. Therefore, not only the magnitude, but also the spatial distributions of the potential predictability of ENSO have heavily dependence on decade. At the same time, since the center of positive correlation represents the region of strong interaction between wind anomalies and SSTA, comparison of Fig. 3a and Fig. 3b can also verify the fact that ENSO may have different evolution characteristics in different decades (Wang, 1995).

4. Potential predictability of interannual climate in mid-high latitudes and Asian monsoon

a. Interannual climate over the Pacific-North America

The most salient atmospheric oscillations on interdecdal timescale of the northern hemisphere

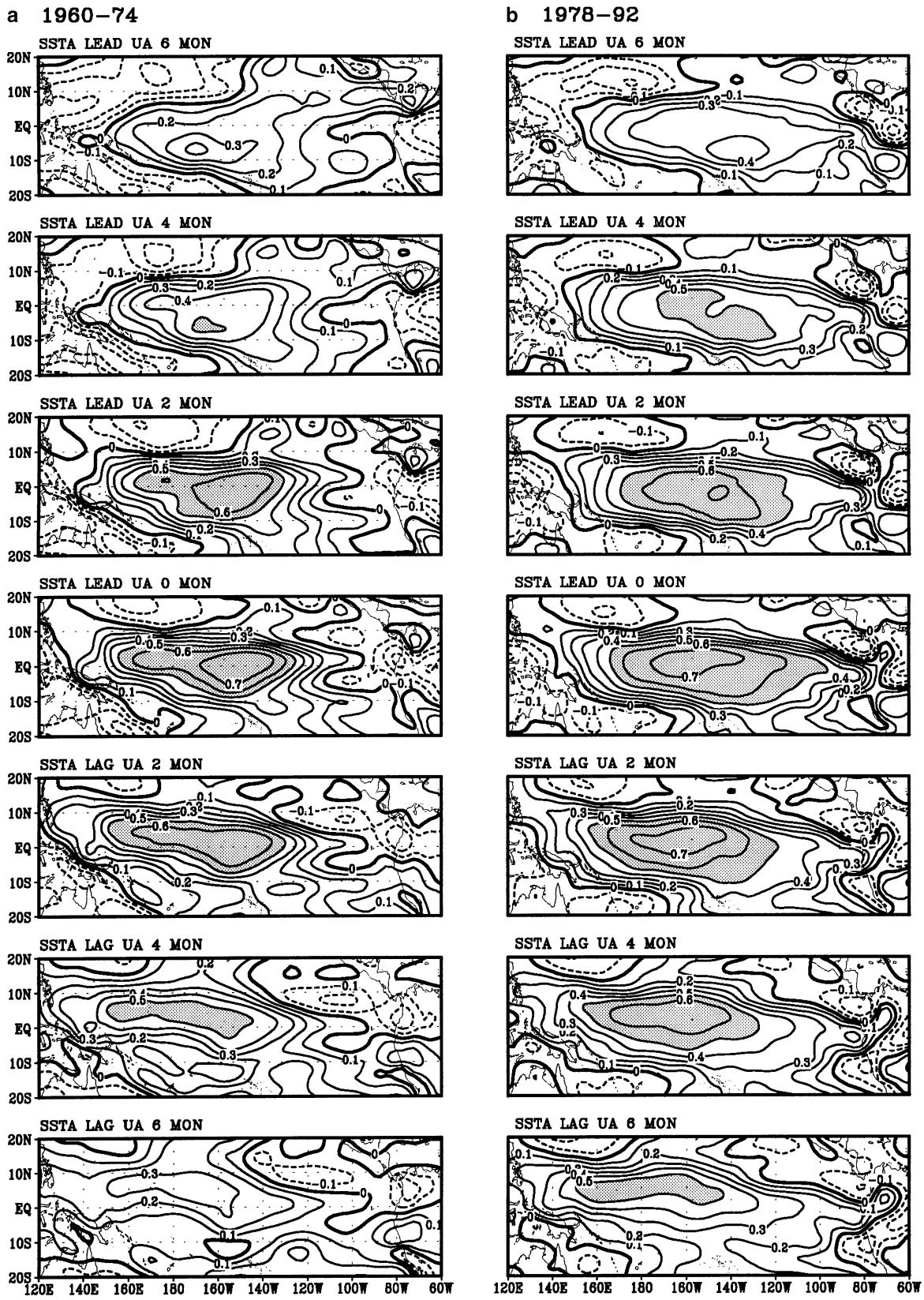

Fig. 3. Distribution of the correlation between monthly zonal wind anomalies at 850hPa and *Nino3 index* during **a.** 1960–64 and **b.** 1978–92. 7 panels from top to bottom represent SSTA leads wind anomalies 6, 4, 2, 0 months, SSTA lags wind anomalies 2, 4, 6 months sucessively. Areas where the correlation is larger than 0.5 are shaded

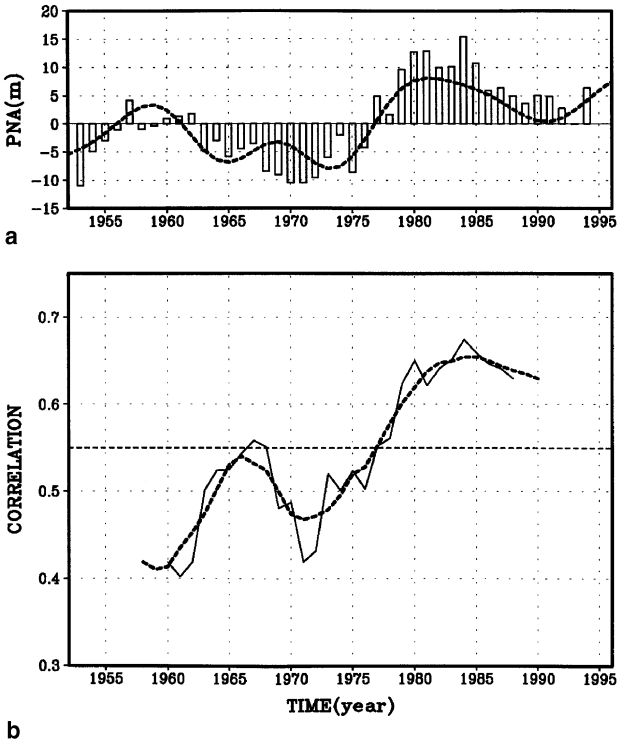

Fig. 4a. 9-year running average and low-pass-filtered series of *PNA index* on interdecadal timescale shown with the vertical bars and the thick dashed line, respectively; **b.** Moving-window contemporary correlation between *PNA index* and *Nino3 index* shown with solid line. Its 5-year running mean is shown with the thick dashed line. The length of moving window is 21 years

are North Altantic Oscillation (NAO) and North Pacific Decadal Oscillation (PDO, Trenberth and Hurrel, 1994). It has been mentioned by many studies that the sea level pressure (SLP) in the North Pacific has long term variations and SLP after 1976 is anomalously low, i.e., the Aleutian low is anomalously strong. *PNA index* is often used to describe the interannual variability of atmospheric circulation of the north hemisphere in boreal winter. With NCEP 500hPa height, *PNA index* from 1949 to 1998 is calculated. From both the 9-year running mean (vertical bars in Fig. 4a) and the low-pass-filtered series (thick dashed line in Fig. 4a), it can be clearly seen that *PNA index* has obvious interdecadal variation with negative anomaly during 1960–76 and positive anomaly after 1978. Exactly as for *Nino3 index* and *TW2 index*, 1977 is a shift point of *PNA index* on interdecadal timescale.

Moving-window contemporary correlation between *PNA index* and *Nino3 index* from 1950 to 1998 is calculated (length of window is 21 years) and shown with solid line in Fig. 4b. The dashed line in Fig. 4b denotes 5-year running average of the correlation. Although the head and tail 10-year correlation are truncated by calculation of the moving correlation, we still can see the significant decadal variation of the potential predictability. Correlation is relatively low before 1976, especially in early 1960s. It increases quickly from 1970 and exceeds 95% significance level ($R_{0.05} = 0.55$) after 1977 and reaches its maximum around 1985. As a whole, the potential predictability in 1980s is obviously higher than that in 1960s and 1970s.

b. The Indian summer monsoon

The inverse relationship between the central-eastern equatorial Pacific SST anomalies (e.g. Nino3 SST) and the Indian monsoon rainfall has been mentioned in many studies (e.g., Shukla, 1987). There are several ways to describe the Indian summer monsoon. For instance, many people use the summer precipitation to measure the variation of the Indian monsoon (Shukla, 1991). In this paper, we use the area-averaged zonal wind shear between 850hPa and 200hPa as a monsoon index. The anomaly series of the Indian monsoon index (*INMI*) is shown in Fig. 5a with vertical bars. Its 9-year running mean and low-pass-filtered series are shown with the dashed line and solid line, respectively. We can see that, during the period from 1950 to 1967 *INMI* is positive implying the Indian monsoon was stronger than normal. *INMI* is negative in 1970s and early 1990s meaning the Indian monsoon was weaker than normal. *INMI* is slightly positive from 1978 to 1987. 1978 is one of the shift points of *INMI* on interdecadal timescale.

Moving-window contemporary correlation between *INMI* and *Nino3 index* is shown in Fig. 5b (length of window is 21 years). It can be found that the correlation coefficient is entirely negative (exceeding 95% significance level) and has obvious decadal variation. The maximum negative value appears in early 1960s (−0.85) then increases to −0.68 in 1975. It rises continuously after 1978 and reaches its maximum value around 1984 (−0.57), then declines quickly after 1985. Since we care the absolute

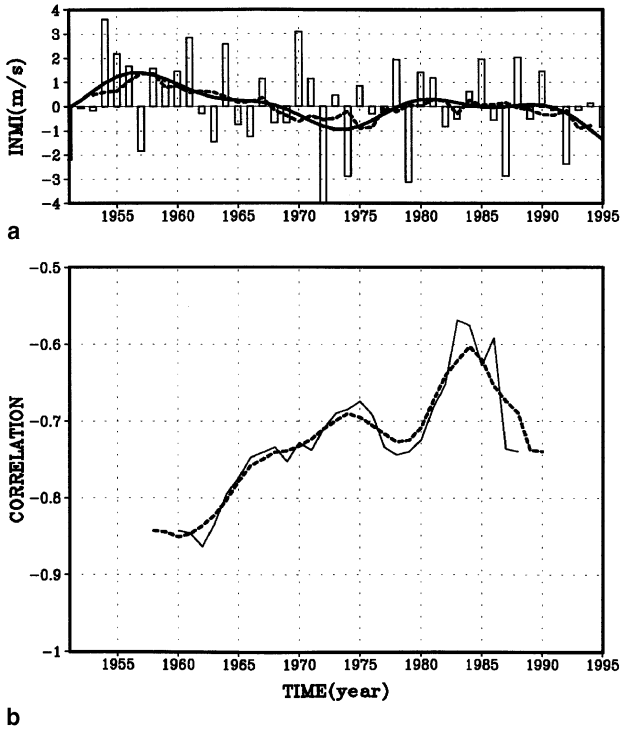

Fig. 5a. Time evolution of the anomaly of Indian monsoon index (*INMI*) shown with the vertical bars. Its 9-year running mean and low-pass-filtered series on interdecadal timescale are shown with the dashed line and the solid line, respectively; **b.** Moving-window contemporary correlation between the *INMI* anomaly and *Nino3 index* shown with the solid line. Its 5-year running mean is shown with the thick dashed line. The length of window is 21 years

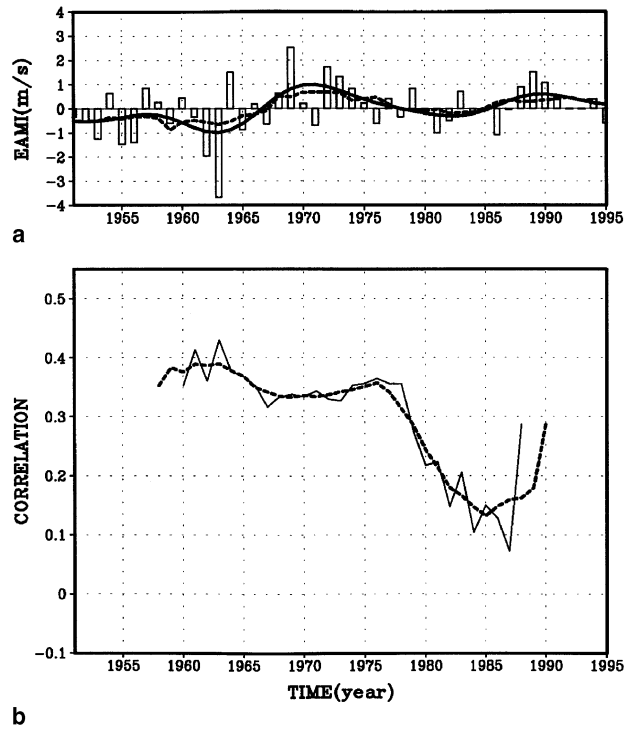

Fig. 6. As Fig. 5 but for the East Asian winter monsoon

value of correlation coefficient, it is easily to be seen that, if Nino3 SST is used as a predictor of the Indian monsoon, the Indian monsoon in early and middle 1980s is relatively more difficult to predict than in 1960s, 1970s and 1990s. This result is quite different from those mentioned in Sect. 3 and Sect. 4a.

c. The East Asian winter monsoon

In the recent years, the interaction between Asian monsoon and ENSO has caused certain attention. Li (1988) pointed out that, in the winter prior to the onset of El Niño the East Asian winter monsoon is anomalously strong, while in the winter during El Niño the East Asian monsoon is often anomalously weak. With NCEP 850hPa meridional wind in boreal winter, the East Asian monsoon index $(EAMI_{win})$ is calculated and its anomaly variation is shown in Fig. 6a with vertical bars. Both the 9-year running mean (dashed line) and the low-pass-filtered series (solid line) indicate that the East Asian winter monsoon is anomalously strong before 1966 and in early 1980s ($v' < 0$), while it is anomalously weak from 1967 to 1977 and after 1987 ($v' > 0$). 1977 is one shift point of $EAMI_{win}$ on interdecadal timescale.

Similarly, moving-window contemporary correlation between $EAMI_{win}$ and *Nino3 index* is calculated and shown in Fig. 6b (length of window is 21 years). It can be seen that correlation coefficient is entirely positive, which implies that during El Niño (La Niña) the Asian winter monsoon is anomalously weak (strong). Although the value of correlation is smaller than that between *INMI* and *Nino3 index*, its decadal variation is notable. Correlation coefficient is relatively high before 1976. But it drops quickly after 1977 and reaches its minimum around 1985, then recovers in late 1980s. Therefore the Nino3 SSTA related potential predictability of the East Asian monsoon is relatively lower in 1980s than in 1960s and 1970s. 1977 is the time when the potential predictability drops rapidly.

d. The East Asian summer monsoon

The East Asian summer monsoon is distinct from the Indian monsoon in both their large-scale structure and constituent subsystems (Lau and Li, 1984; Tao and Chen, 1987). Following the definition of *EAMI* with use of meridional wind at 850hPa in summer (July), we can get the East Asian summer monsoon index ($EAMI_{sum}$) and its anomaly. As shown in Fig. 7a, it is interesting that even without any filtering or time averaging (vertical bars), the interdecadal variation of $EAMI_{sum}$ is very apparent with positive anomaly before 1974 (except for 1967, 1968 and 1972) and negative anomaly after 1976. The 9-year running mean (dashed line) and low-pass-filtered series (solid line) indicate more clearly interdecadal variability of the East Asian summer monsoon. The result is consistent with Guo (1983) although he used another definition of the East Asian summer monsoon index.

Moving-window lagged correlation between $EAMI_{sum}$ and *Nino3 index* ($EAMI_{sum}$ lags *Nino3 index* 6 months) is shown in Fig.7b. It can be found that the coefficient is low, which suggests that the effect of Nino3 SSTA is only a partial cause of the interannual variation of the East Asian summer monsoon. However, the correlation shows obvious decadal variation. It is low before 1970 but rapidly increases from 1972 to 1976. After 1976, the correlation decreases to about 0.2. As a whole, the potential predictability of the East Asian summer monsoon is relatively higher in the middle and late 1970s than in other periods.

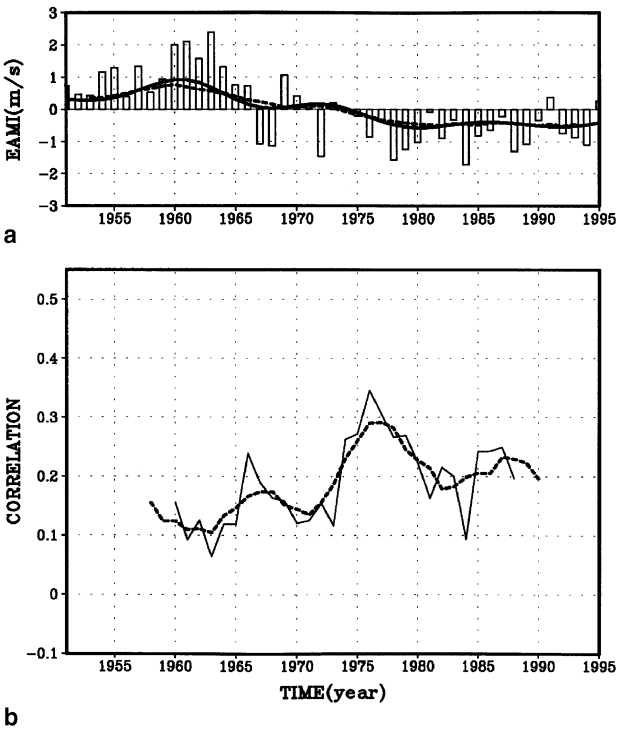

Fig. 7. As Fig. 5 but for the East Asian summer monsoon and in Fig. 7b $EAMI_{sum}$ lags *Nino3 index* 6 months

5. Concluding remarks

A number of important indices such as *Nino3 index, TW2 index, PNA index, INMI, EAMI* were used to indicate the interdecadal variation of the tropical Pacific SST, wind and atmospheric circulation over mid-high latitudes and Asian monsoon. Autocorrelation of *Nino3 index* and moving-window led/lagged correlation between *Nino3 index* and other indices were applied to investigate the decadal changes of the potential predictability of ENSO and interannual climate anomalies. The main results are summarized as follows:

a. Interdecadal variability exists not only in the tropical Pacific SST but also in the tropical Pacific wind field, mid-high latitude atmospheric circulation and Asian monsoon. On interdecadal timescale 1977 is a shift point for many climate indices. For example, Nino3 SST shifts from cold to warm, the equatorial zonal wind anomalies from eastward to westward, *PNA index* from negative to positive and the East Asian winter (summer) monsoon from weak (strong) to strong (weak).

b. Autocorrelation of *Nino3 index* and correlation between atmospheric indices and *Nino3 index* exhibit significant decadal variation, which suggests that Nino3 SSTA-related potential predictability of ENSO and interannual climate anomalies possesses distinct decadal changes. ENSO and the atmospheric circulation over the Pacific-North America (PNA) in boreal winter are more predictable in 1980s than in 1960s and 1970s. The potential predictability decreases in 1990s. In contrast, Nino3 SSTA-related potential predictability of the Indian summer monsoon and the East Asian winter monsoon is lower in 1980s than in 1960s and 1970s.

c. 1977 is not only a shift point for the climate state as summarized in *a*, but also a catastrophe point of the potential predictability of ENSO and interannual climate anomalies. There is always a dramatic changes (increase or decrease) in correlation coefficient near 1977.

d. Besides the time-variation of the magnitude, the potential predictability has apparent decadal variation in its spatial distribution and propagating characteristics.

Although the tropical Pacific is relatively warmer after 1977 and the potential predictability of ENSO is higher in 1980s than that in 1960s and 1970s, that is not to say that the predictability of ENSO is necessarily higher in a warmer decade than in a colder decade. As a matter of fact, many models exhibit lower prediction skill in 1990s, while it is generally accepted that the tropical Pacific is in a strong warm state after 1990. The present study and many numerical models only reveal the decadal variation of the potential predictability of ENSO and interannual climate anomalies without any dynamical explanation of (i) why there is always an abrupt increase or decrease of the potential predictability near 1977? Why ENSO is more predictable in 1980s while Asian monsoon is less predictable? (ii) why ENSO and its potential predictability exhibit different propagating characteristics in different decades? what are the dominant mechanisms? To answer these questions, much work need be done in the future.

Acknowledgments

This research was supported by NSFC 49906003.

References

Balmaseda M, Davey M, Anderson D (1995) Decadal and seasonal dependence of ENSO prediction skill. J Clim 8: 2705–2715

Barnett T (1991) The interaction of multiple time scales in the tropical climate system. J Clim 4: 269–285

Cane M, Zebiak S, Dolan S (1986) Experimental forecasts of El Niño. Nature 321: 827–832

Chen D, Zebiak S, Busalachi A, Cane M (1995) An improved procedure for El Niño forecasting: Implications for predictability. Science 269: 1699–1702

CLIVAR. A study of climate variability and predictability. Science Plan. August 1995, WCRP-89, WMO/TD, No. 690, 1996

Flugel M, Chang P (1998) Impact of the seasonal cycle on the ENSO prediction. J Atmos Sci 55: 3230–3243

Gu D, Philander S (1995) Secular changes of annual and interannual variability in the tropics in the past century. J Clim 8: 864–876

Guo Q (1983) Analysis on the East Asian summer monsoon intensity indices and its variation. Acta Geographica Sinica 38(3): 207–216

Ji M, Leetmaa A, Kousky V (1996) Coupled model forecasts of ENSO during the 1980s and 1990s at the National Meteorological Center. J Clim 9: 3105–3120

Latif M, Barnett D, Cane M, Kleeman R, Leetmaa A, O'Brien J, Rosati A, Schneider E (1998) A review of the predictability and prediction of ENSO, J Geophy Res 103(C7): 14375–14392

Lau K, Li M (1984) The monsoon of East Asia and its global association – A survey. Bull Amer Meteor Soc 65: 114–125

Li C (1998) Frequent activities along the East Asian trough and the formation of El Niño. Sci in China(b), 667–674

McPhaden M (1999) Genesis and evolution of the 1997–98 El Niño. Science 283: 950–954

Ni Y (1993) Climate Dynamics, The Meteorological Press of China, p50–51

Qian W, Zhu Y, Ye Q (1998) The interannual and interdecadal variability of the central to eastern equatorial Pacific SST anomalies. Chinese Science Bulletin 43(10): 1098–1102

Shukla J (1987) Long range forecasting of Indian monsoons, Science Age, Nov 1987, pp 21–23

Shukla J (1991) Short term climate variability and prediction, In: Proc. Second world climate conference. Jager J and Ferguson H (eds). Cambridge University Press.

Tao S, Chen L (1987) A review of recent research on the East Asian summer monsoon in China. Monsoon Meteorology, Chang C and Krishnamurti T (eds.), Oxford University Press, pp 60–92

Trenberth K, Hurrel J (1994) Decadal atmosphere-ocean variations in the Pacific. Clim Dynm 9: 303–319

Trenberth K, Branstator G, Karoly D, Kumar A, Lau N, Ropelewski C (1998) Progress during TOGA in understanding and modeling global teleconnections associated with tropical sea surface temperatures. J Geophy Res 103(C7): 14291–14324

Wallace J, Gutzler D (1981) Teleconnection in the geopotential height field in the northern hemisphere. Mon Wea Rev 109: 784–812

Wallace J, Rasmusson E, Mitchell T, Kousky V, Sarachik E, Storch H (1998) On the structure and evolution of ENSO-related climate variability in the tropical Pacific. L Lessons from TOGA. J Geophy Res 103(C7): 14169–14240.

Wang B (1995) Interdecadal changes in El Niño onset in the last four decades. J Clim 8: 267–285

Webster P, Yang S (1992) Monsoon and ENSO, Selective interactive systems. Quart J Roy Meteor Soc 18: 877–926

Zhang R, Sumi A, Kimoto M (1996) Impact of El Niño on the East Asian monsoon: A diagnostic study of the ′86/87 and ′91/92 events. J Meteor Soc, Japan 74(1): 49–62

Authors' address: A. Wu and D. Hu, Lab of Ocean Circulation and Air-sea Interaction, Institute of Oceanology, Chinease Academy of Sciences Qingdao 266071, P. R. China.